JA

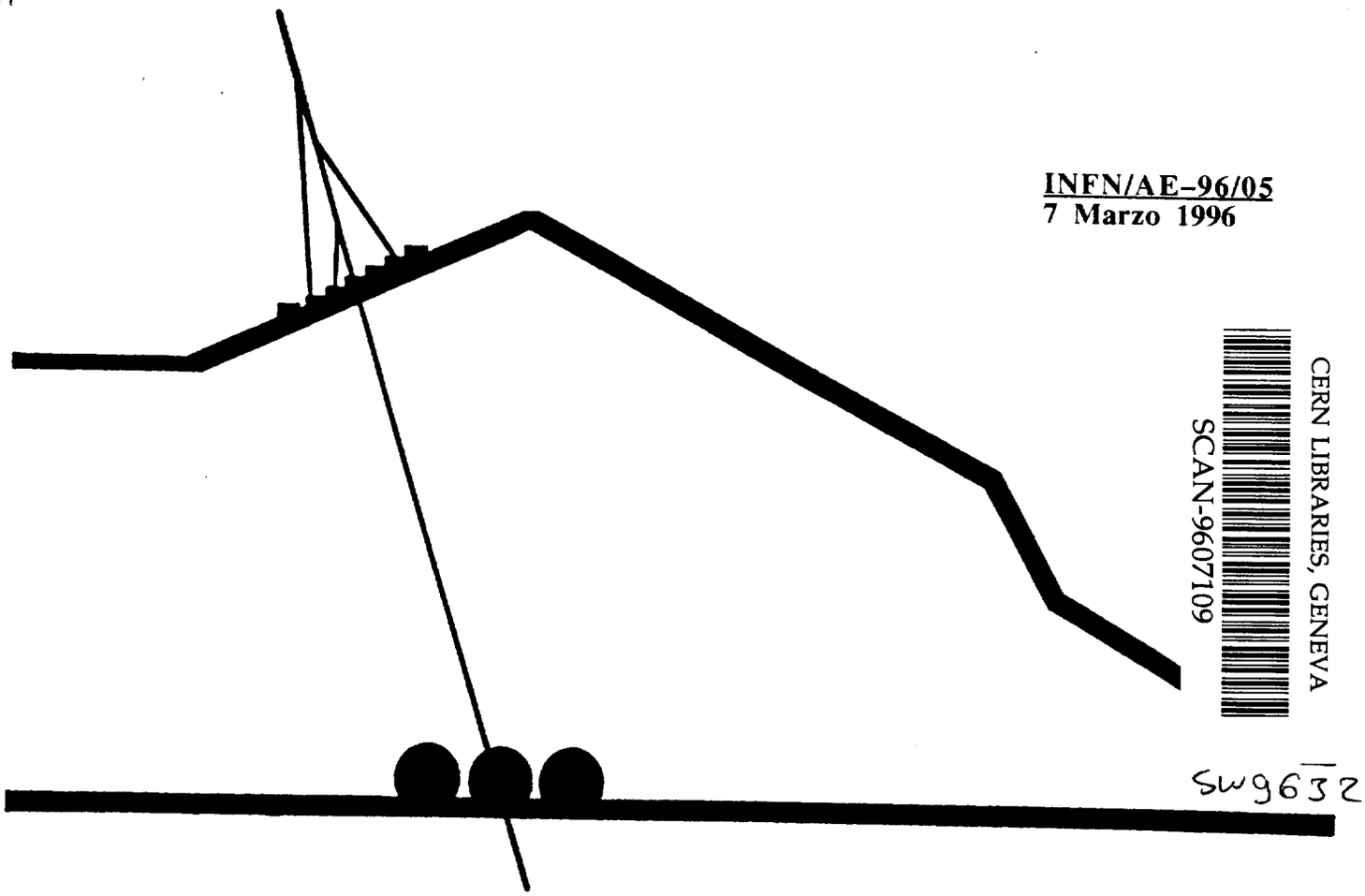

INFN/AE-96/05
7 Marzo 1996

SW9632

INTRODUCTION TO HIGH ENERGY COSMIC RAY PHYSICS

G. Battistoni, A.F. Grillo

(Lectures given by G. Battistoni at the Fourth Trieste School on "Non Accelerator Particle Astrophysics")

INFN - Laboratori Nazionali del Gran Sasso

Published by **SIS–Pubblicazioni**
dei Laboratori Nazionali di Frascati

INFN - Istituto Nazionale di Fisica Nucleare
Laboratori Nazionali del Gran Sasso

INFN/AE-96/05
7 Marzo 1996

INTRODUCTION TO HIGH ENERGY COSMIC RAY PHYSICS

G. Battistoni[1], A.F. Grillo[2]

[1] INFN–Sezione di Milano, Via Celoria 16, I–20133 Milano, Italy

[2] INFN–Laboratori Nazionali del Gran Sasso, ss 17 bis Km 18+910, I–67010 Assergi L'Aquila

1 Introduction

The topic of cosmic rays is very wide, and is deeply related to many fields of physics, ranging from astronomy to nuclear physics and elementary particles. In the framework of the program of a school on non-accelerator particle astrophysics, these short lectures are thought to provide an introduction to the subject of the nuclear component of cosmic rays, and its relation with a few relevant issues of astrophysics and particle physics. Such a program can be accomplished under different points of views: here, we undoubtely try to present the matter as it is seen with the eyes of a high energy particle physicist. Indeed, we cannot forget that the present particles physics has taken origin from the observations and the measurements on cosmic rays performed in the first half of our century, from the discovery of positron, in 1932, to that of Σ^+, in 1953. Now, when the physics at accelerators is starting to fight against both technological and also financial limitations, we see that new interest is flowing back to the origins. In fact, many stimulating and unresolved questions are still presented to us by the nuclear cosmic radiation, and this is particularly true for the extremely high energies.

The main open questions of astrophysical interest can be summarized in the fact that almost one century after their discovery, we have no definitive models about the origin, acceleration and propagation processes of cosmic rays, while we recognize that they bring information about the surrounding universe, our Galaxy for sure, and very probably also the extragalactic space, at least at the highest observed energies. Of particular importance is the question of their acceleration, since the present observations show that, as compared to the known technologies, the amount of organisation (i.e. efficiency) delivered in the energy transfer to comic rays is exceptionally high. Many astrophysics objects are considered as candidate cosmic accelerators: from Super Nova remnants or binary stellar systems to Radio Galaxies or Active Galactic Nuclei. Besides that, there is also discussion on the possible role played in the acceleration by the topological defects relics from the first stages of our Universe: this has brought to the attention of physicists also the possible connections between cosmic rays and cosmology. From the point of view of particle physics, we have to remind that we are able to observe the cosmic rays of the highest energies only through their interaction with the Earth's atmosphere. The reliability of our interpretation of the features of such secondary particles, and of their relation to the characteristics of the primary particle, is necessarily related to quality of our understanding of hadron-hadron, hadron-nucleus and nucleus- nucleus interactions. This aspect is particularly stimulating for high energy physicists, since there is not yet an exact way to calculate the properties of the bulk of hadronic interactions. Also, from the experimental point of view, the productions of secondary cosmic rays at very high energies occurs in kinematic regions, or energy ranges, that have not been explorated in accelerator experiments, and that will hardly be accessed at the hadron colliders of the next generation. Here, after a few general qualitative considerations about the known characteristics of primary cosmic rays arriving at the top of atmosphere, as given in Section 2, we shall briefly mention the fundamental concepts on propagation (Section 3) and acceleration (Section 4) of Cosmic Rays. A short review of the experimental situation, both from direct and indirect experiments is given in Section 5. In Section 6 we shall resume some concepts on the hadronic interactions at high energy, in order to apply them to the production of secondary particles in atmosphere, which will be treated, in a simplified but analytical model, in Section 7. As remarked above, we shall stick, almost everywhere, to the high energy sector. In practice we shall neglect the energy region (at the GeV scale and below) which is normally affected by solar modulation effects.

2 Generalities and Fundamental Observational Results

This is not a place for a review of the historical milestones in the comprehension of cosmic rays (for which we recommend, for instance ref.[1, 2, 3, 4, 5]). However, let us remind here a few important steps achieved since the first decades of our century. The first important recognition was the extra-terrestrial origin of cosmic rays. The evidence for that came mainly through the following observations:

- The increase of the induced ionization in air as a function of height, together with its decrease underground or underwater, consistently with an attenuation process in the Earth's atmosphere

- The decrease of the induced ionization as a function of latitude, consistently with the interaction of charged particles with the geomagnetic field. We now can state that, in order to reach sea level from the vertical, in the dipole geomagnetic field, a charged particle must have a magnetic rigidity R such that:

$$R = \frac{cp}{Ze} \geq 15cos^4\,(latitude)\,(GV) \tag{1}$$

  For instance, at 40° latitude, a proton needs at least a rigidity of 5 GV (corresponding to an energy of about 4.3 GeV), to reach the earth's surface.

- An east-west effect is also present, with the ionization increasing looking west with respect to the vertical, consistently with the fact that cosmic ray particles are mostly positive.

More than that, it was also recognized that only a small part of cosmic rays arriving to the earth are of solar origin, while the bulk of cosmic rays flux has to come from regions outside the solar system. The main facts in favour of this conclusion are:

- the essential isotropy of the arrival directions when measured in sidereal coordinates

- the non observation of a decrease in flux during eclipses

- the detection of an anti-correlation (in some region of the energy flux), with the solar activity consistently with the hypothesis of particles penetrating, from outside the solar system, into the solar wind.

Staring form the 50's, a major attention was paid to the astrophysics questions arising from cosmic rays. The main topic concerns the sites and mechanism of particle acceleration. We want to mention the argument, invoked be Ginzburg[6], who showed how the power available from Super Novae explosions could be used for cosmic ray acceleration (see below). Then, with the birth of radio-astronomy, it was found how the radio emission was consistent with the emission of waves from synchrotron radiation by relativistic electrons[7]. A prediction of the power spectrum from radio to visible light was also possible, for instance for the emission from the Crab Nebula (coming from the explosion of SN1054A[4]).

Very shortly, at present we know that cosmic rays, at sea level are mostly $\mu^{\pm}$, $e^{\pm}$, γ, a few hadrons and many ν's. The integrated flux of charged particles at sea level is of the order of 200 $m^{-2}s^{-1}$. We understand them as "Secondary Cosmic Rays" produced by the interaction of "Primary Cosmic Rays" with the earth's atmosphere. Such primaries, at the top of atmosphere, are made of protons (~90%), He nuclei (~9%) and other nuclei (~1%), up to the Iron nuclei, for an integrated flux of about 1000 $m^{-2}s^{-1}$. There are also primary electrons (e/p = ~ 1%) and photons (γ/p = ~ 0.1%).

One of the striking features of cosmic rays, and in particular of the dominant nuclear components, is their energy spectrum, which extends through many energy decades, with little, if any, structures. In this respect, let us remind here some terminology that can be useful in the following. We can distinguish, for simplicity of discussion, different energy ranges:

- the High Energy (HE), in the GeV region: ($1\ GeV = 10^9\ eV$)
- the Very High Energy, in TeV the region: ($1\ TeV = 10^{12}\ eV$)
- the Ultra High Energy, in the PeV region ($1\ PeV = 10^{15}\ eV$):
- the Extreme High Energy, in the Eev region and beyond ($1\ EeV = 10^{18}\ eV$).

From the experimental point of view, there are events measured up to a few 10^{20} eV, corresponding to a flux of $\sim 1\ km^{-2} century^{-1}$!. The first relevant quantity to which we are interested are the energy spectra. They can be expressed as differential flux (number of particles in the range E, E+dE), or integral flux (number of particle with energy exceeding or equal E). There are different ways of measuring, or defining, a flux, in the relevant literature, usually reflecting different experimental aspects.

1. The "All Particle Spectrum", namely the number of particles (nuclei) as a function of total energy E_0. This is best suited to describe the results of experiments which do not detect the nature of the primary particle, and for calorimetric measurements.

2. The number of particles (nuclei) as a function of Energy/nucleon (E_0/A), where A is the mass number of the nucleus. Since nuclear processes (spallation) approximately conserve E_0/A, this is a way to study the interaction of nuclei in the propagation in the interstellar medium (see section 3).

3. The number of nucleons as a function of Energy/nucleon. Since the nuclei with mass number A and energy E_0 interact approximately as a beam of A independent nucleons of energy E_0/A, this is a useful way to follow the production of secondary particle, such as muons in earth's atmosphere or neutrinos in stellar atmosphere (see Section 4).

4. The number of particles as a function of magnetic rigidity R. This is well suited to study confinement and acceleration of cosmic rays, since both process are probably due to the interaction with static or variable magnetic fields.

In Fig. 1 a compilation of the all particle primary spectrum is shown, starting from the TeV region (the data marked "Proton-4" are measurements performed on the primaries outside the atmosphere from a satellite experiment, while all other points come surface detectors measuring secondary particles), while in Fig. 2 (taken from ref.[2]) the all-nucleon spectrum of the main mass components is plotted, including the lowest energy region. The energy range below 10 GeV is affected by solar modulation, while at higher

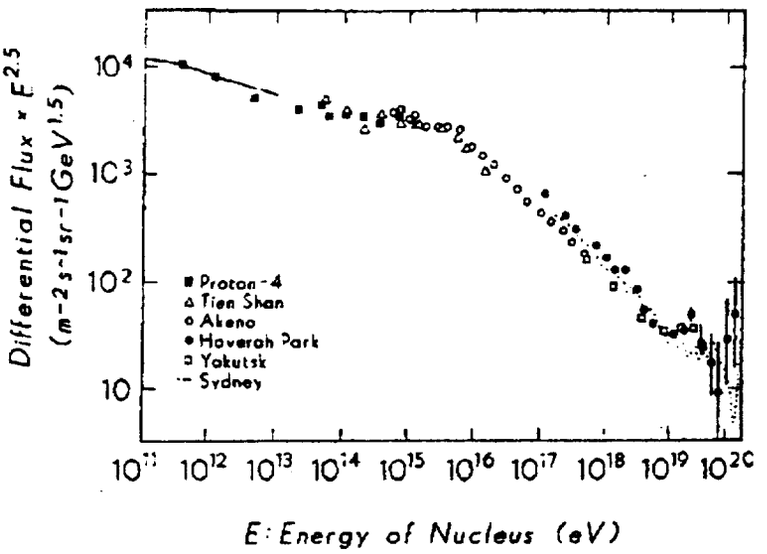

Figure 1: The all-particle spectrum of cosmic rays for energies exceeding 0.1 TeV.

energy particles are more "rigid" and such "local" magnetic effects can be neglected. In this notes we shall not discuss the low energy sector.

The high energy spectra exhibit an extreme regularity. It is conceivable that different physical processes are involved in the production, acceleration and transport of cosmic rays, but they apparently conspire to produce a smooth power spectrum of the kind $E^{-\gamma}$. The all-nucleon differential spectrum is well approximated by:

$$\frac{dN}{dE} = 1.8(E/GeV)^{-2.7}[nucleons/m^2 \cdot sr \cdot s \cdot (GeV/A)] \tag{2}$$

at least below PeV energies. There are some peculiar but well defined features which break the apparent regularity: in the PeV region there is a "knee" where the spectral index, γ changes from ~ 2.7 to $\sim 3.0 \div 3.1$. At about 10^{19} eV the spectrum seems to flatten again, determining the so called "ankle". Both the knee and the ankle are considered as relevant hints in the understanding of the physical processes at the origin of primary cosmic rays.

Knowing the flux, we can define an energy density of cosmic rays, assuming that these are uniformly and isotropically distributed in the space region around us (say, our galaxy).

$$\rho = \frac{4\pi N(\geq E)}{\beta c} \approx 1\ eV/cm^3 \tag{3}$$

Considering that the energy density of star light is about 0.6 eV/cm^3, and that of the galactic magnetic field (whose average value is about 3 $\mu Gauss$) is 0.26 eV/cm^3 we understand how the cosmic ray share great part of the total energy available around us. For exercise, if we extrapolate such density homogeneously to the rest of the Universe (even if there are no experimental evidences that really authorize such an extrapolation!), we end

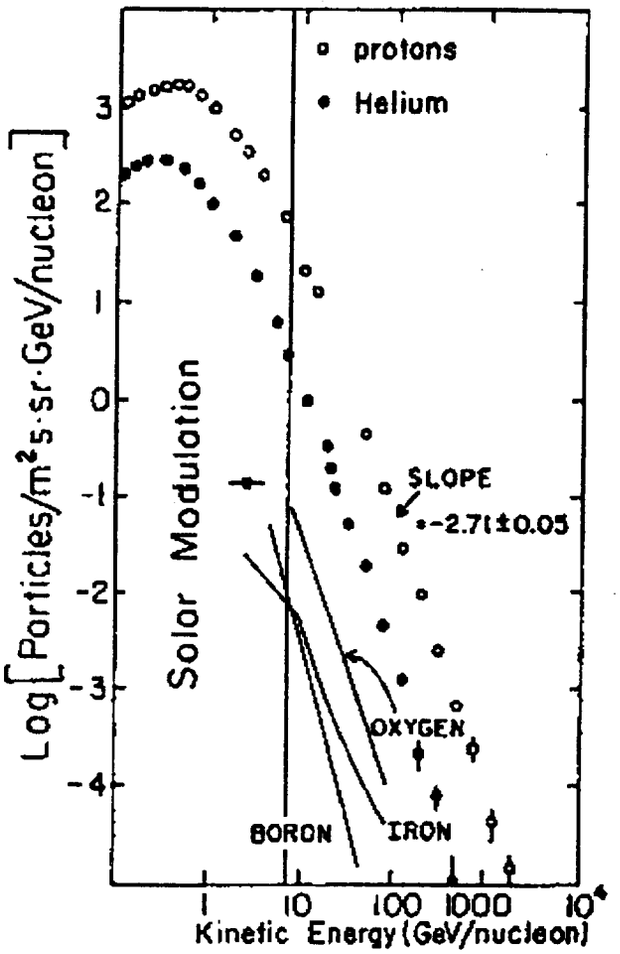

Figure 2: Compilation of the all-nucleon spectrum of different mass components. The energies below the vertical line are those which are deeply affected by solar modulation.

up finding that cosmic rays are about 1% of the total mass of the Universe, so that they would represent by far the most important energy transformation process of the Universe.

3 The Nature of Cosmic Ray and their Propagation in the Galaxy

The chemical abundance of elements in cosmic rays is known, at least up to a a few tens of TeV/nucleon, from the results of the observations performed at high altitude or in space. A general agreement with the abundances found in Solar System has been detected, with the exception of some nuclei, as shown in Fig. 3, which even being extremely rare in stellar evolution, are more abundant in cosmic rays.

These are interpreted as secondary products of nuclear spallation processes occurring

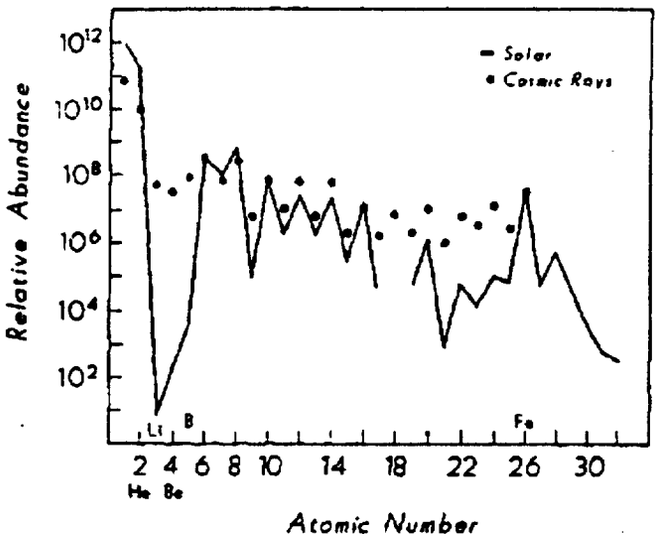

Figure 3: Distribution of the relative abundances of chemical elements in the solar system and in cosmic rays.

in the interactions of heavier nuclei with the protons of the interstellar medium ρ_{ISM}, whose value is about 1 hydrogen atom/cm^3. We can describe this process as:

$$A + p \rightarrow A^* \tag{4}$$

with A^* fragmenting in lighter nuclei. Such a reaction, as a first approximation, conserves E/A (known as "straight-on" approximation, for a more precise discussion see [8]). Thus, nuclei as C and O are likely to produce secondary Li, Be and B, while Fe can originate Sc, V, Ti or Mn. The question is: what is the amount of material that cosmic rays must cross in order to produce the observed abundances of secondary nuclei, without depleting too much the primary abundance itself? The evolution of abundances can be described by Transport Equations. In a simple system in which only two species exist, primaries (N_p) and secondaries (N_s), and assuming that the only way the particle number changes is through spallation processes, we can write the following system

$$\begin{aligned} \frac{dN_p}{dX} &= -\frac{N_p}{\lambda_p} \\ \frac{dN_s}{dX} &= -\frac{N_s}{\lambda_s} + \frac{N_p P_{sp}}{\lambda_p} \end{aligned} \tag{5}$$

where X is the amount of crossed material in g/cm^2, λ_i are the interaction length for the specie i, and P_{sp} is the probability of producing a given secondary from the spallation of a primary nucleus, which is in practice the ratio $\sigma_{spallation}/\sigma_{total}$. The values of these last two parameters have to be deduced by experimental data from accelerators. Solving the

system 6, the ratio of secondary to primary abundance as a function of the amount of crossed material is:

$$\frac{N_s}{N_p} = \frac{P_{sp}\lambda_s}{(\lambda_s - \lambda_p)}\left[exp\left(\frac{X_{sp}}{\lambda_p} - \frac{X_{sp}}{\lambda_s}\right) - 1\right] \tag{6}$$

For example[1], if we consider as primary the medium mass group (C-N-O, $\lambda_{CNO} \sim 6.7\ g/cm^2$, and as secondary product the light group (Li-Be-B, $\lambda_{LiBeB} \sim 10\ g/cm^2$, the observed ratio is about 0.25, and using the experimental spallation cross sections we get P_{sp}=0.35. Then, the best estimate the amount of crossed material, X_{sp}, is 4.3 g/cm^2.

Of course, this is a very simplified picture, and more general systems of coupled equations can be written, also including time-dependent evolution (see below) and the presence of many different species. However, even in this approximation, one is able to arrive at quite remarkable results. The value obtained for X_{sp} allows us to evaluate the total time (space) length that cosmic ray spend (travel) between the source and their arrival on earth, assuming that they are mostly confined inside our galaxy. Very schematically, we can approximate our galaxy as a disk of radius $R = 15kpc$, and thickness $D = 300pc$, and making the hypothesis that the matter density in the inter-galactic space is much less than that of the interstellar medium around us ($\rho_{ISM} \sim 1\ H\ atom/cm^3$). It can be easily seen that cosmic rays must travel along a path of the order of 1 Mpc, corresponding to confinement time of about $3 \cdot 10^6$ years, which is much longer than the time to cross straightly the disk thickness: the contribution of possible secondary production in intergalactic medium is entirely negligible, even with extreme assumptions on intergalactic density[1]. Summarizing, we are brought to consider the following scenario:

- some particles (nuclei) are produced and accelerated somewhere;
- There exists some mechanism that confines such accelerated particles in a confinement volume, possibly identified as our Galaxy;
- During the propagation phase, these particles produce the observed abundances of light elements, through the interactions with the InterStellar Matter.

Let us see how a general formalism can be established to describe the propagation process. This is accomplished by the "Diffusion-Loss Equation"[6]. For the i-specie of cosmic ray particle such equation is:

$$\begin{aligned}
\frac{dN_i(E,X,t)}{dt} &= Q_i(E,X,t)\ \ (source\ term) \\
&+\vec{\nabla}\cdot\left(D_i\vec{\nabla}N_i(E)\right)\ \ (Diffusion) \\
&-\frac{\partial}{\partial E}\left[\frac{dE}{dt}N_i(E)\right]\ \ (Energy\ variation) \\
&-\vec{\nabla}\cdot\vec{u}N_i(E)\qquad (Convection) \\
&-\left(\frac{v_i\rho\sigma_i}{m_n}+\frac{1}{\gamma_i\tau_i}\right)N_i(E)\ \ (loss\ by\ interaction\ and\ decay) \\
&+\frac{v_i\rho}{m_n}\sum_{k\geq i}\int\frac{d\sigma_{ik}(E,E')}{dE}N_k(E')dE'\ \ (prod.\ of\ (i,E)\ by\ (k,E'))
\end{aligned} \tag{7}$$

Notice that N_i and Q_i are differential in energy. Such an equation is fairly general and can describe transport in any medium: interstellar matter, earths atmosphere or Stellar atmosphere. According to the physical process under consideration, or to the required approximations, some terms of the equation may be dropped: Eq. (5) is just a very simplified example in the assumption of stable nuclei and interaction through spallation processes which conserve E/A.

Before entering into further description, it is better to remind some more detail about our Galaxy. Approximately, we can say that the effective volume of the Galaxy is $V_g \simeq 2 \cdot 10^{66}\ cm^3$, filled, apart from matter, with a magnetic field whose average value is about 3 $\mu Gauss$. This field has not the same orientation everywhere, but instead gives rise to domains, whose linear extension is the $3 \div 10\ pc$ range. The $\vec{B}$ orientation is almost uniform inside each domain, but the orientation is also randomly distributed among the different domains. Let us also remind that if $\vec{B}$ is inside a plasma (gas of ionized particles) with negligible resistivity, then it is straightforward to show that the phenomenon of "flux freezing" takes place: the field moves with the plasma. In this environment, charged particles perform a kind of random walk, being effectively confined, and this suggests a magnetic origin for cosmic ray confinement. Then, there is another experimental information that is necessary to consider: the relative fraction of secondary to primary nuclei that we quoted above, is an average value dominated by the flux at low energy. Indeed the N_s/N_p ratio decreases as a function of energy. This suggests that acceleration is separated from propagation, and that the escape probability is energy dependent, in agreement with the idea that confinement has a magnetic origin, so that a dependence on magnetic rigidity is expected.

If the mechanism depicted has some reality, then at higher energies, cosmic rays should be less and less isotropized by the propagation: this trend is apparently shown (although with large errors) by the experimental data, suggesting that the knee itself is somehow related to the escape probability.

After all these observations and deductions, the simplest phenomenological model which accomodates them is the so called "Leaky Box" model. Its main assumption is that particles diffuse freely in a confinement volume, from which they can escape with a probability which is independent on time, but which is (possibly) dependent on Energy. This brings to an exponential distribution of the path lengths. If we just consider only the diffusion term, then

$$\frac{dN_i}{dt} = -DN_i \quad \left(D = \frac{1}{\tau_{escape}}\right) \tag{8}$$

From which we get

$$N_i(t) = N_0(t)e^{-t/\tau_{esc.}} = N_0(x)e^{-x/\lambda_{esc.}} \tag{9}$$

Now, if we consider the steady state at equilibrium ($dN/dt \equiv 0$), the Diffusion-Loss equation takes the form:

$$\frac{N_i}{\tau_{escape}} = Q_i - \left(\frac{\beta_i c\rho}{\lambda_i} + \frac{1}{\gamma_i \tau_i}\right) N_i \tag{10}$$

For a primary stable nucleus (like a proton, for instance) we drop the production and

decay terms, and we arrive to the following expression:

$$N_p = \frac{Q_p \tau_{esc}(E)}{1 + \lambda_{esc}(E)/\lambda_p} \tag{11}$$

Instead, for stable, pure secondaries (*i.e.* $Q_i \equiv 0$), we have:

$$N_s = -\frac{\beta_i c \rho \tau_{esc}}{\lambda_s} N_s + \frac{\beta_i c \rho \tau_{esc}}{m_n} \sigma_{sp} N_p \tag{12}$$

So that we obtain:

$$\frac{N_s}{N_p} = \frac{\lambda_{esc}/\lambda_p P_{sp}}{1 + \lambda_{esc}/\lambda_s} \tag{13}$$

which describes how the ratio of secondaries to primaries depends on energy through λ_{esc} It is possible to write various coupled equations for the transport: this allows to fit τ_{esc} as a function of the rigidity R or of the energy. Under the simplest hypothesis that τ_{esc} is the same for all nuclei, the typical fit results give $\lambda_{esc} \simeq 11 \ \ g/cm^2$ for $R < 4 \ \ GV$, and $\lambda_{esc} \simeq 11 \ g/cm^2 \ (4/R)^\delta$ for higher R, with $\delta = 0.6$. Going back to the propagation of primaries, in the case of protons we notice that $\lambda_p \sim 55 \ g/cm^2$ is greater than λ_{esc}, so that, for $E > 4 \ \ GeV$

$$N_p(E) = Q_p(E)\tau_{esc}(E) \propto Q_p(E)E^{-\delta} \tag{14}$$

Since we know from observations that the differential proton flux arriving on earth goes as $E^{-\gamma} \simeq E^{-2.7}$, we can deduce that at source level one should have:

$$Q_p(E) \propto E^{-\gamma+\delta} \simeq E^{-2.1} \tag{15}$$

On the other hand, in the extreme case of Fe nuclei, $\lambda_{Fe} \sim 2.6 g/cm^2 << \lambda_{esc}$, so that we can expect that $N_{Fe}(E) \propto Q_{Fe}(E)$. Therefore, even if the same mechanism is responsible for the acceleration of the different nuclear components, we should observe different spectral index at observation level for each nuclear mass group. As an example of the success of the Leaky Box model, in Fig. 4 we show the fluxes of different primary elements, measured during a Space Shuttle mission, as compared to a propagation calculation based on such model.[9].

4 The acceleration mechanisms

The question of the sites where acceleration of cosmic rays takes place, and that of the acceleration mechanisms, is still an open question of extreme astrophysical (and general) interest, together with the full understanding of the propagation processes. In the framework of this introductory lecture, we cannot include a comprehensive review of this topic. As for the discussion of propagation and confinement, we prefer to quote the most important achievements reached so far in this matter and to point out the major question under debate, making reference to the specialized literature.

One important step in the modelization of cosmic ray acceleration came from the work of Ginzburg and Sirovatsky[6], who associated the acceleration process to the Super Novae

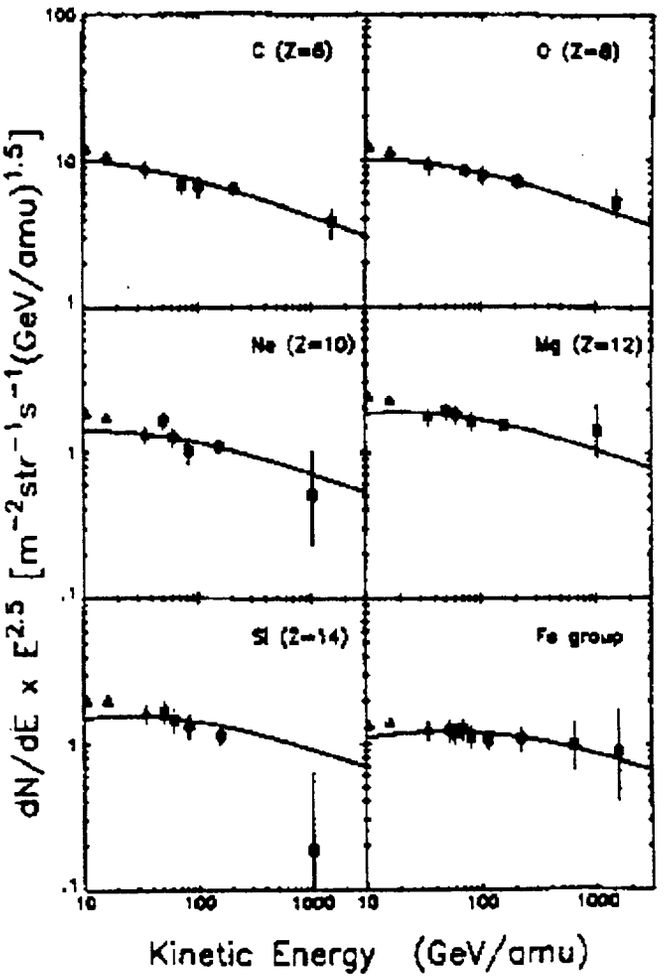

Figure 4: Measured energy spectra of some primary nuclei compared with the results of a propagation calculation based on the Leaky Box model.

explosions, using an "order-of-magnitude" argument, which considers the following steps. First of all, let us define the Luminosity L_{CR} of the Galaxy in terms of cosmic rays:

$$L_{CR} = \frac{\rho_E^{c.r.} V_g}{\tau} \tag{16}$$

where, using the figures quoted in the previous sections. $\rho_E^{c.r.} \sim 1\ eV/cm^3$, $V_g \sim 2 \cdot 10^{66} cm^3$, and $\tau \sim 10^6 y \simeq 3 \cdot 10^{13}\ s$, then $L_{CR} = 10^{41} erg/s$. If we consider a typical Super Nova remnant (Crab), the radio observation allows to estimate the kinetic energy of accelerated electrons, which turns to be around $10^{47}\ erg$. We expect this to correspond to about 1% of the kinetic energy of the protons, that is $\sim 10^{49}\ erg$, if we assume that the value of e/p in the terrestrial environment is general. Therefore, if the Super Novae rate is $\simeq (30\ y)^{-1}$, as mainly deducted from the observation of distant galaxies, the corresponding luminosity L_{SN} would assume the value of $3 \cdot 10^{40}\ erg\ s^{-1}$, in reasonable agreement with L_{CR}.

This is just an energy balance argument, and one should look at the possible dynamics of the acceleration mechanism. In general, charged particles acceleration is achieved by means of e.m. processes. We cannot expect the constant electric fields could play a role in that, due to the fact that in a plasma, having a negligible resistivity, such fields cannot exist. Instead, the electric field associated to variable magnetic fields is a more realistic possibility. In this respect, it would be natural to consider fast rotating pulsars (neutron stars) as typical cosmic accelerators. In fact, if we take the case of a young pulsar, the magnetic field at the surface can be of the order of $B \simeq 10^{12}\ G$, and the rotation period is $P \simeq 10\ ms$. If the magnetic axis forms an angle with respect to the rotation axis, then we have a rotating magnetic dipole whose luminosity can be of the order of $L = 2 \cdot 10^{39}\ erg\ s^{-1}\ (P/10\ ms)^4$. Only $10 \div 100$ of these object would be enough to give account of the total cosmic ray luminosity, and since the maximum energy achievable would be of the order of $E_{max} \sim Bc$, then the limit of $10^{20}\ eV$ would be also achieved.

However, these are again plausibility considerations: the possibility of maintaining such a field in a plasma, the necessity of transferring rotational energy to the accelerated particles, and the fact the severe losses are expected, makes the matter far from trivial.

At present, the most successful description of the acceleration for the bulk of cosmic rays (up to about $10^{14}\ eV$), is the one related to shock waves from Super Novae. Qualitatively speaking, such an acceleration originates from the energy transfer of a moving macroscopic body (here the shock wave from the Super Nova explosion) to the elementary particles or nuclei existing in the interstellar medium, after many, small steps in which energy variation occurs. Let us describe this shock wave as a plane wave front of magnetized plasma propagating itself with a certain speed, $\vec{u}_1$. The (relativistic) particles, assumed to be already present in the interstellar medium, undergo scatterings from the magnetic structures of the expanding front in which they exchange momentum but do not lose energy ("collisionless" scattering).

The interesting thing is that the energy gain in such a process appears as a consequence of relativistic boosts from different frames, as follows from the following considerations. In the collision of the particle with the shock front, which can be considered as a macroscopic moving "mirror", the c.m. frame, in practice, is the rest frame of the mirror itself. In this frame, we have that in each scattering only $\Delta\vec{p}^{\star} \neq 0$, while $\Delta E^{\star} = 0$. However, if we consider the process in the laboratory frame, which is the galaxy rest frame, we can have an energy gain after the Lorentz transformation in all those cases in which the incoming particle is back-scattered with respect to the original direction. Let us see in detail a simplified example: a particle of energy E and momentum $\vec{p}$, arrives perpendicularly against a plane shock mirror moving with speed $\vec{v}$ (and corresponding Lorentz factor γ) towards the particle. In the c.m. frame the particle will have energy $E^{\star} = \gamma(E + vp)$ and momentum $p^{\star} = \gamma(p + \frac{v}{c^2}E)$. In this frame, after the collision, $E_1^{\star} = E^{\star}$, while $p_{1\star} = -p^{\star}$. Now going back to the galaxy frame, the particle will have energy E_1 given by:

$$E_1 = \gamma(E_1^{\star} + vp_1^{\star}) \simeq E + 2\gamma^2\frac{v}{c}E \tag{17}$$

We have then that for each encounter of this type, the fractional energy increase is $\eta = \frac{1+\beta}{1-\beta} - 1$ at the expenses of the (assumed infinite) kinetic energy of the shock. This is

of course the most convenient case. If one considers a realistic geometry, averaging over all possible angles of incidences, $\eta \sim \frac{4}{3}\frac{u_1-u_2}{c} = \frac{4}{3}\beta$, where $-\vec{u}_1$ is the expansion speed of the plane shock front, and $\vec{u}_2$ is the speed with which the shocked material flows away from the shock, relatively to the shock rest frame. In the case of a strong shock, *i.e.* when its propagation speed is much larger than the typical "sound" speed of the medium (in a plasma this is the Alfven speed[10] c_1), or, in other words, when the "Mach number" M is high: $M^2 = (u_1/c_1)^2 >> 1$, it can be shown that $u_1/u_2 \simeq 4$[11]. A typical order of magnitude for u_1 is $5 \cdot 10^8\ cm/s$.

This acceleration mechanism is known as first order Fermi acceleration[12], who first considered the process of energy transfer from macroscopic regions of magnetized plasma to individual charged particles. The denomination "First Order" comes from the fact that $\eta \propto \beta$, as opposed to the "Second Order", less efficient, acceleration in which $\eta \propto \beta^2$, as it would occur in the encounters with randomly moving magnetized clouds. This last scenario was the one originally considered by Fermi in his original paper, and the different result between First and Second order versions stems just from the different geometries and consequent angular averages.

Going back to the case of the plane front, we see that the application of the First order Fermi acceleration is able to reproduce other appealing features, such as the power law spectrum of accelerated particles. We understand that once a particle crosses the shock has, after each collision, a certain probability $1 - P_{esc}$ to remain in the acceleration region and to be put back in the unshocked region to restart an acceleration cycle having a characteristic duration time T_{cycle}. It can be shown that

$$P_{esc} = \frac{rate\ into\ shock}{rate\ out\ of\ shock} \sim 4\frac{u_2}{c} \tag{18}$$

and that, after a certain number of collisions, if P_{esc} and η are energy-independent, then the integral energy spectrum of the accelerated particles will be of the form:

$$N(> E) \propto E^{-\alpha} \tag{19}$$

where $\alpha = \frac{P_{esc}}{\eta}$ which can be intuitively justified, since in this process a constant fraction of particles is progressively shifted towards energies larger by a constant factor, thus giving rise, at steady state, to a linear relation in a log-log scale. Using the expression given above, we see that $\alpha = \frac{3}{u_1/u_2 - 1} \sim 1 + O(\frac{1}{M^2})$. This is surely interesting, since, as discussed in the previous section, we expect that at source, the integral energy spectrum has to be $Q(> E) \propto E^{-\gamma+\delta+1} \sim E^{-1.1}$.

However, the quoted model cannot be completely satisfactory. For instance, as we stated above, there is an injection problem, since it assumes the existence of relativistic particles before acceleration. Furthermore, and this is the most important shortcoming, there are difficulties in attaining particle energies higher or equal the knee region of the primary spectrum. There are two main parameters determining the maximum energy: one is T_{cycle}, and the other is the total time length for which the acceleration process can be active, T_A. The cycle time length depends on diffusion on both the unshocked and shocked material, which on turn depends on the strength of the magnetic field irregularities trapped in the shock, ultimately responsible of the scattering process.

These assumptions, in the case of a strong shock ($u_2 = u_1/4$), brings to the following B-dependent lower limit for $T_{cycle}(E)$:

$$T_{cycle} \geq \frac{20E}{3u_1 ZeB} \tag{20}$$

. Therefore the rate of energy gain is[13]:

$$\frac{dE}{dt} \propto \frac{E}{T_{cycle}} = \frac{3u_1^2 ZeB}{20c} \tag{21}$$

and considering that the accelerator operates for a finite time T_A, one get a limit for the ultimate energy/particle:

$$E_{max} = \frac{3u_1^2 ZeB}{20c} T_A \tag{22}$$

A guess on the value of T_A is obtainable considering that the shock is active until the density inside it is larger that that of the interstellar medium:

$$\frac{M_{exp}}{4/3\pi(u_1 T_A)^3} = \rho_{ISM} \tag{23}$$

For a typical value of M_{exp} of about 10 solar masses, we have $T_A \sim 10^3\ y$. Therefore, being $B \sim 3\ \mu G$, we get:

$$E_{max} \simeq 30\ Z\ TeV \tag{24}$$

Notice that in this elementary derivation we have neglected unavoidable energy loss processes, and that all the above considerations are valid for typical parameter values. However, we have to admit that acceleration is likely to occur in highly non-typical environments, and some peculiar variation with respect to the quoted numbers cannot be excluded. In particular, if either B or T_A are bigger than our estimates, also E_{max} will grow. In any case we are brought to the following preliminary conclusions:

- Acceleration in Super Novae remnants is possible.
- The associated luminosity would be enough for the bulk of cosmic rays.
- Particles with higher Z will reach higher energies, and only heavy nuclei are expected to reach the knee.
- As a consequence, we expect an enrichment of the fraction of heavy nuclei in the knee region of the primary spectrum. We notice that the same effect can be obtained by rigidity-dependent confinements arguments.

It is fair to add, however, that there is little direct experimental evidence for the validity of this mechanism. The present data [14] are now reaching a sensitivity such as to be able to verify (or falsify) in the next few years this hypothesis.

At the end of this short discussion on the acceleration process, let us remind other possible mechanisms which could explain higher energies:

- Short duration shocks in a high B-field. as possible in pre Super Novae ejecta. In this case a maximum energy of 10^{16} eV is possible.
- Long duration shocks in a low B-field, as can be assumed for the description a Galactic winds. This model can predict up to $3 \cdot 10^{17}$ eV.
- Galactic point sources, with rotational energies $\sim 10^{60}$ $erg(P/10\ ms)^2$, but this would lead to an unrealistic too big luminosity.
- Infall of matter in a compact object, such as binary X-ray sources, which can give an X-Luminosity around $L_X \sim 10^{38}$ $erg\ s^-1$. Here also a maximum energy of 10^{16} eV can be achieved. Only 500 object of this type in our Galaxy would be enough to account for the estimated cosmic ray luminosity.
- Super Novae explosion into the wind of the predecessor object[15]. Presently this is one of the most favoured solutions to explain the acceleration above the knee. Candidate objects are the so called Wolf-Rayet stars.

All these quoted hypotheses are however insufficient to account for the highest observed energies (from 10^{18} to more than 10^{20} eV). Here the matter is more speculative. and the theoretical research is oriented in the following directions. with some preference for extra-galactic models:

1. A re-acceleration process of some kind
2. Accretion onto Galactic size objects, such as Active Galactic Nuclei (AGN).
3. Not independently from the above point, the Radio Galaxies are also good candidates.
4. Finally, there is the possibility of the decay of heavy objects of cosmological origin (cosmic strings or other topological defects)

To conclude this section, we emphasize how the comprehension of the acceleration (as well as of the propagation) of cosmic rays is far from being reliably understood. In order to arrive to a general clarification of these aspects. it is therefore crucial to measure with the best possible accuracy the energy spectra. the elemental composition, and their evolution with particle energy of primary cosmic rays, expecially from the knee region, up to the highest observable range.

5 Short Review of Experimental Data: Direct and Indirect Measurements

We can roughly divide the experimental methods adopted to measure fluxes and chemical compositions into two large categories: "direct" and "indirect" measurements. The direct measurements are those who detect and identify directly the primary particles. Therefore

they have to be performed at high altitude (high mountains, stratospheric balloons, satellites), since the atmosphere would behave as a shield. Due to the difficulties induced by the experimental condition (constraints on the space and on the weight of the payload), such measurements have given well established results up to about 10^{12} $eV/nucleon$, for which a relatively small "aperture" (defined as the acceptance measured in $m^2 \cdot sr$) is enough to perform a significant measurement in a limited time period (typically, a single balloon flight can last up to $10 \div 15$ days). More recently, there have been results for the low mass components up 10^{14} eV[17].

At higher energies instead (knee region and beyond), the flux is so low that the only chance is to have earth-based detectors of large area, operating for long times. In that case, the atmosphere is considered as a target, and one studies the primary properties in an "indirect" way, through the measurement of secondary particles produced in the atmosphere.

Let us review, very shortly, the main achievements from direct measurements. Roughly speaking, there are three kind of detectors:

- Totally passive detectors (emulsions, track-etch plastics, etc.).
- Totally active detectors, that is using devices providing electronically processable signals (wire chambers, Cherenkov light detectors, semiconductor detectors, calorimeters with different technologies, etc.). As examples we can quote the apparata for satellites or space shuttle, such as CRN[16] (see Fig. 5), or for the future space stations.
- Mixed (passive+active detectors) apparata, and a typical example is the the JACEE experiment[17], whose sketch is given in Fig. 6.

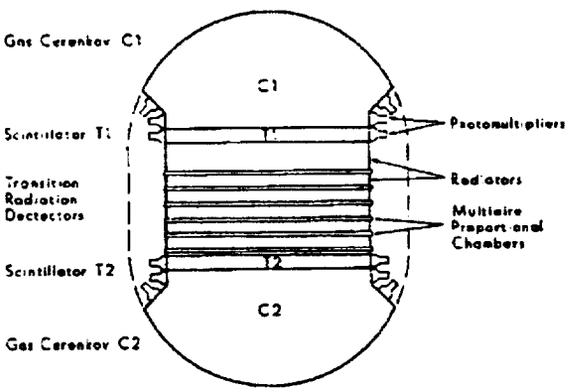

Figure 5: The Chicago University experimetal set–up.

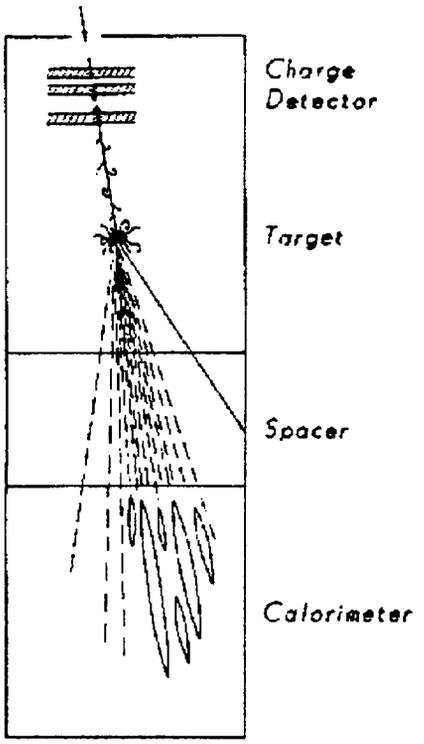

Figure 6: A schematic representation of the JACEE experimental set–up.

In Figg. 5 and 5. we show a compilation of the results from different direct experiments. combined for 5 mass groups[18]. A fit to the measured fluxes for the all different nuclei can be found in ref.[19], up to 1 $TeV/nucleon$.

In summary, after grouping the different nuclei in a few mass groups, from the lightest one (protons) up to the very heavy (Fe nuclei), one finds that all these components, individually, can be fitted by the usual power law spectrum, but the spectral index varies. This reinforces the conclusions that either acceleration or propagation (or both) mechanisms affect in different ways the different nuclear species. When considering the average values for the spectral indices, the heavy components exhibit a flatter spectrum, therefore the global compositions becomes heavier with increasing energy. These results are usually well in agreement with the predictions coming from the hypothesis of acceleration by Super Novae, and from the predictions of the leaky box model, as far as the propagation effects are concerned[20].

These results are valuable, and have to be assumed someway as a normalization basis for all the indirect experiments. More questionable are the results obtained by the direct experiments near the 10^{14} eV region. Here the nature of primary particles can be still identified with an acceptable confidence range. However, the energy assignment is now indirect since it is generally based on the energy deposition of particles produced in the interaction of primaries in the detector itself. The reconstruction of the total energy is then obtained by comparison with some model prediction, and therefore, at least in that

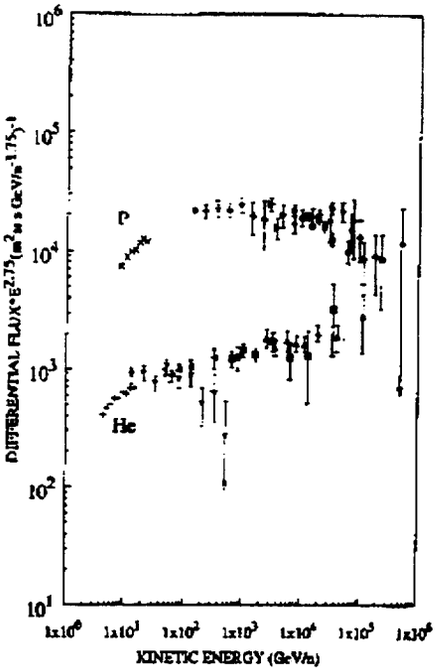

Figure 7: Compilation of flux data for Hydrogen and Helium components from different direct experiments.

region. the boundary line between "direct" and "indirect" experiments is more uncertain.

Entering now in the field of indirect measurements, it is convenient to summarize here the main properties of the earth's atmosphere, which has to be considered now as a nuclear target and a calorimeter (≡total absorption detector) at the same time. The chemical composition of earth's atmosphere is well established up to a very large height above the sea level. For our purposes we just remind here that it is dominated by nitrogen.and, since it is relevant for the interaction of primary particles, its average mass number is $\langle A \rangle = 14.7$. One of the most important features to take into account is density evolution as a function of height: $\rho = \rho(h)$. The amount of matter (column density) seen by a primary cosmic ray arriving from the vertical direction would be:

$$X_v = \int_0^\infty \rho(h)\, dh \tag{25}$$

In the approximation of an isothermal atmosphere, $\rho(h)$ has an exponential behaviour, and the same shape has therefore the vertical depth, which we describe as:

$$X_v = X_0 e^{(-h/h_0)} \tag{26}$$

where h is the height above the sea level, $h_0 \sim 6.4\ km$ and $X_0 \sim 1030\ g/cm^2$. More realistic parameterizations exist, taking into account also the differences for the specific

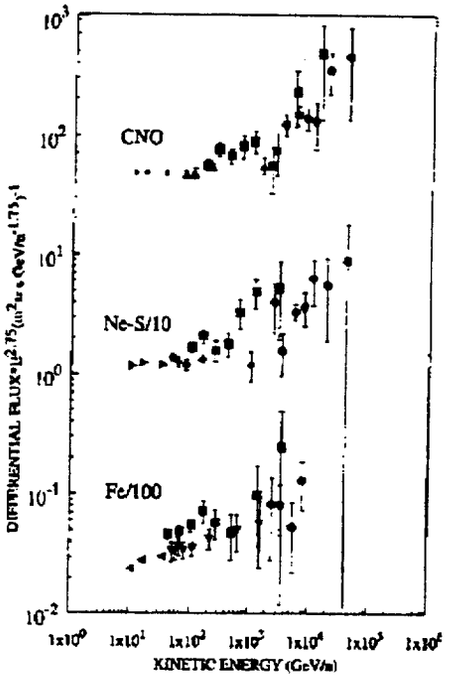

Figure 8: Compilation of flux data for medium-heavy and heavy mass groups from different direct experiments.

geographic sites. In case of incidence with zenith angles (*i.e.* angles with respect to the vertical) larger than 60°, the earth' s curvature can be neglected, and the actual slant depth is just $X = X_v/cos(zenith)$. For larger zenith angles it is relatively easy to get the proper expression, and this is left to the reader as an exercise.

Let us describe qualitatively what happens when a primary nucleus interacts in the high atmosphere. In average, within one "interaction" length, λ_A, the nucleus starts breaking into fragments, and this fragmentation continues until the nucleus breaks into nucleons. This has to be described by detailed nuclear models; however, for most purposes, in particular at high energy, we can rely on the simple Superposition model: a nucleus of mass number A and total energy E_0, behaves as a beam of A independent nucleons each one having energy E_0/A and interaction length λ_N. Each nucleon will interact with the target nuclei of the atmosphere producing many hadrons in the final state. Each hadron particle will go on interacting again with the atmosphere or decaying into other particles. At very high energy the typical interaction length of a nucleon in air is about 80 g/cm^2, while a heavy nucleus can interact after only few g/cm^2. We have then the evolution of a hadronic shower of particles, which develops completely since the atmosphere is ≈ 13 interaction lengths deep, for protons. At each initial step in the shower process the number of particles will grow while the average energy will decrease. Thus, the number of particles (or, with less ambiguities in the definition, the quantity of energy transferred

to secondaries and eventually released in the atmosphere) will reach a maximum at some depth which is a function of energy, of the nature of the primary particle (as stated before, the first interaction of a Fe nucleus occurs in the average much earlier that that of a proton) and of the details of the interactions of the primaries and secondaries in the cascade (see section 7). After that, the energy/particle is so degraded (will be below some "critical energy") that energy losses dominate over particle multiplication process, and the shower "size" will decrease as a function of depth: it grows "old". The critical energy is process dependent: for instance, for low energy electrons the relevant energy is that at which energy losses by ionization become important, while for e.g. underground muons is the energy necessary to produce a muon capable to penetrate the rock through the detector.

Most of the produced particles in each hadronic interaction are π and K mesons. Charged pions (and kaons) can decay into muons (and neutrinos) before interacting, thus producing the most penetrating component of the atmospheric showers. Neutral pions decay immediately into photons which initiate electro-magnetic showers (the radiation length in atmosphere is about 37 g/cm^2, and the critical e.m.energy of 81 MeV), made of electrons, positrons and photons.

These atmospheric showers are known as Extensive Air Showers (EAS). Their longitudinal evolution is a function of the nature and energy of the primary particle. Their lateral extension depends on the average transverse momentum of the hadronic component, and, in the case of the electro-magnetic component (which, speaking in number of particles, is the most important one) it is strongly affected by the multiple Coulomb scattering. A dedicated review of the EAS properties can be found in these proceedings[21].

The e.m. component allows different types of measurements. By means of surface arrays (typically using scintillator detectors modules scattered over a large area), it is possible to sample the amount of e.m. particles (usually defined as "shower size") arriving at earth at a given depth in atmosphere, fixed by the height of the array above the sea level and by the zenith angle. For a given direction, and therefore for a given thickness of atmosphere, it is possible to determine E_0, and maybe A, by means of dedicated simulation tools describing the hadronic interaction and the shower evolution. A more powerful determination of mass composition can be achieved by measuring the correlation between different components. For instance: Number of e^+e^- vs the number of muons and/or hadrons, at a given atmospheric depth. This can be easily understood in the framework of the superposition model. Cascades induced by heavier nuclei develop and attenuate faster than proton induced showers of the same energy, because they have less energy per nucleon. Nucleons of lower energy produce mesons which also have lower energies, and these decay more often than high energy ones, thus giving rise to more muons. On the other hand, the rapid attenuation of cascades arising from lower energy pions results in less electrons (positrons) in the lower part of the atmosphere. Muons and hadrons can be identified by tracking detectors. These EAS arrays sample only a part of the shower, but may reach an extremely large area, up to many km^2. The schematic layout of one EAS array, the Yakutsk experiment[22], detecting both the e.m. component (by means of scintillation counters) and the Cherenkov light of the showers, is shown in Fig. 7.

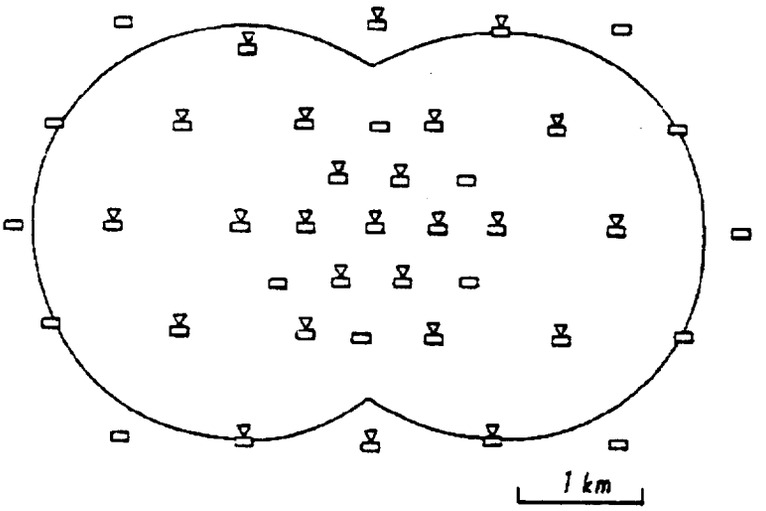

Figure 9: Layout of the Yakutsk array. Rectangles represent scintillation counters, while triangles are Cherenkov counters. The solid line represents the 90% triggering efficiency area of tha array.

As an example of a modern giant array we may quote the AGASA detector[24] which encloses an area of about 100 km^2 and has been able to detect events up to $3 \cdot 10^{20}$ eV. Such apparata can operate continuously. Most of our knowledge of the all-particle spectrum from the knee region up to the extreme high energies comes in fact from the e.m. EAS arrays (see Fig. 1). There are systematic differences in the results of different experiments, and they are probably connected to different detector systematics or possible different criteria for defining the shower size, and to different $N_{e^+e^-} \leftrightarrow E_0$, model-dependent, conversion methods. The conclusions concerning the chemical composition in the knee region and above, from the analyses of the correlation of the different EAS components, are not yet conclusive and still controversial[23]. An interesting question concerns the maximum observable energy. It has been suggested that the interaction of nuclear particles with the photons of the microwave background in the Universe, through the process $\gamma(3\ K)\ p \rightarrow \pi p$, with a threshold at $4 \cdot 10^{19}$ eV can give rise to a cut-off, known as the Greisen-Zatsepin-Kuzmin cut-off[26]. If the extreme high energy components are of extra-galactic origin, there they must travel for at least $\sim 100 Mpc$. Only protons would survive (heavier nuclei would be fragmented) and only for a maximum energy just around $10^{20}\ eV$. Recent analyses[25] seem to give some evidence for the existence of this cut-off.

Electrons and positrons (the lightest particles) in their propagation in the atmosphere, are also able to produce Cherenkov light, when their energy exceeds 35 meV. This light is emitted in a narrow cone along the shower axis. It can be detected by telescopes of photo–multipliers which are able to operate mostly during dark nights. They are mainly used up to the TeV energy region.

The ionizing component of the EAS can also induce fluorescence radiation (in the

visible spectrum) from the excitation of the N_2 molecules of the air. The photon yield is limited with respect to the Cherenkov radiation, and the efficiency is low, but has the advantage that it is emitted isotropically and has a relatively low absorption coefficient in atmosphere. This allows the construction of omni-directional telescopes of photo-multipliers which cover quite a large effective area. Furthermore, it is possible to measure the longitudinal shower profile, also identifying the atmospheric depth of the shower maximum. These features give important constraints in the determination of primary energy and composition, but the interpretation of data is always somewhat dependent on shower models. Also, the understanding of systematics associated to the experimental detection of fluorescent light is not a trivial question. The first one of these detectors is the Fly's Eye experiment [27]. It operates with an energy threshold in the EeV range, up to the maximum observable energy. The recent analysis of Flys Eye data[28] point out that in the range $10^{17} \div 10^{18}$ eV the primary composition should be heavy, and only at the ankle a proton component would become again dominant, suggestive of an extra-galactic component in cosmic rays above 10^{19} eV. Of course, these results need further confirmation by other experiments.

The penetrating muon component can be investigated by underground detectors. There, the rock overburden shield the low energy particles and the (small) surviving hadron component. By selecting muons of energy in the TeV region (corresponding to rock thickness of the order of 1 km), in practice one is sensitive to the secondary hadrons produced in the early stages of the VHE and UHE showers, that is particles which carry the remainder of the first interaction features. This kind of underground detection can thus provide information about the primary features, including in particular the chemical composition, for the reasons already quoted above. This kind of experimentation has acquired some relevance only in the last few years, after the constructions of very large underground detectors. The physics of underground muons is presented in the dedicated lectures that can be found in these proceedings[29].

In order to have a better understanding of the secondary particle production in the atmosphere, in the following sections we shall review some properties of the hadronic interactions at high energy. This will also help to understand some simplified analytical treatment of the shower in atmosphere.

6 A Short Summary on the Hadron Interactions

The basic ingredients for the understanding of showers are the total cross section nucleon-Air (and in general hadron-Air, related to the interaction length) and the differential cross section for multiparticle production. When we speak of total cross section, we should better specify that we are interested in the inelastic part of it, since elastic scattering does not contribute to the processes relevant for our problem. More fundamental than the nucleon-nucleus cross section is the nucleon-nucleon one, since the first can be obtained in terms of the second. In order to understand that, let us consider a primary proton colliding with a nucleus of A nucleons. Due to the short range of hadron interaction, the proton will interact with only some of nucleons of the target. The number of such "wounded"

nucleons can be estimated by simple geometrical considerations considering the path of the projectile inside the nucleus. The main relevant parameters are the cross section (the "orthogonal effective area") of the proton, the size of the nucleus and its nuclear density. At high energy, since the binding energy of a nucleon is only of the order of 8 MeV, the incoming proton interacts independently with each of these wounded nucleons. All this is mathematically described by the Glauber multiple scattering formalism[30]. In that treatment, we end up with an expression for nucleon-nucleus (and nucleus-nucleus) cross section which is just a function of σ_{pp}. In Fig. 8 the total and inelastic σ_{pp} is plot as a function of beam energy. Asintotically, the elastic part should become comparable to the inelastic one.

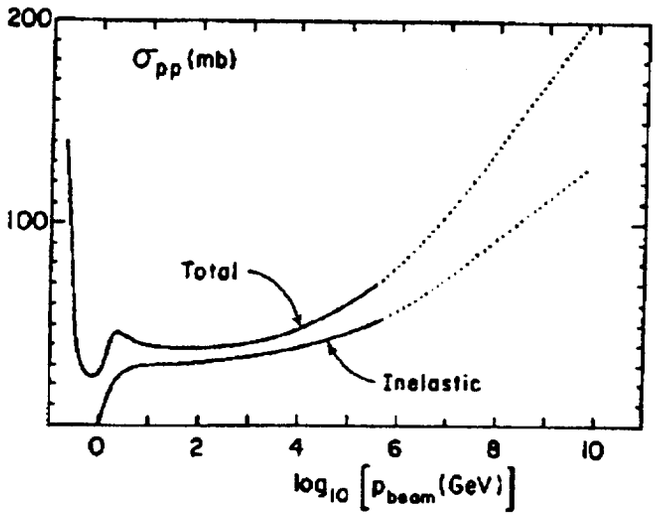

Figure 10: The total and inelastic proton-proton cross section as a function of beam energy.

A compilation of σ_{pAir} is instead given in Fig. 9. The continuous curve is the result of a calculation, the black data points come from the Fly's Eye [27] and Yakutsk[22] experiments, while the boxes represent the measurements of the Akeno EAS array[31]

The multi-particle production in hadronic interactions such as $p+A \rightarrow 1+2+3+...+n$ can be described in terms of exclusive cross sections. In the case of the production of exactly n particles:

$$\frac{d^3\sigma}{dp_1^3...dp_n^3} \tag{27}$$

which are proportional to the probability of finding particle number 1 in the momentum range $p_1 \leq p \leq p_1 + dp_1$ and the particle number 2 in $p_2 \leq p \leq p_2 + dp_2$ ... and the n-particle in $p_n \leq p \leq p_n + dp_n$. These cross section can be made Lorentz when expressed

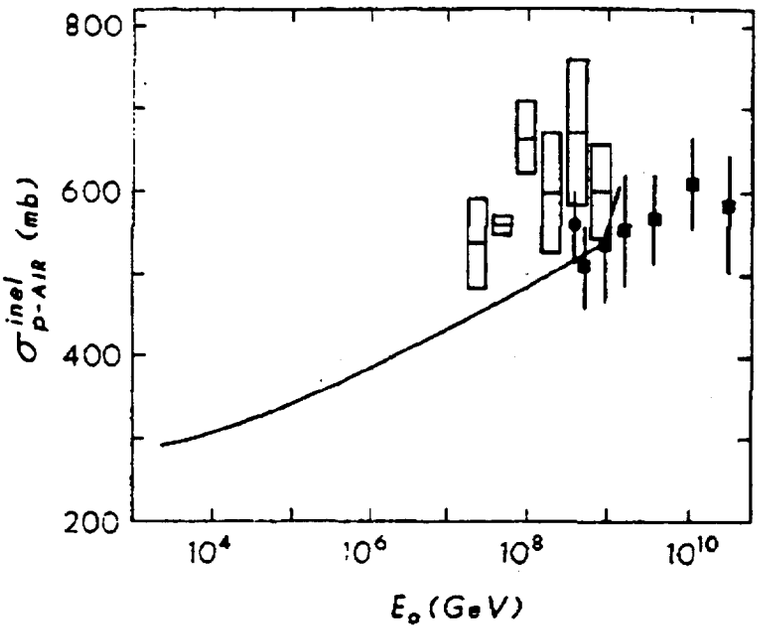

Figure 11: The calculated and measured proton-Air cross section as a function of incident energy.

as:

$$E_1 ... E_n \frac{d^3\sigma}{dp_1^3 ... dp_n^3} \tag{28}$$

since both σ (which has the meaning of an area orthogonal to the beam direction) and dp^3/E are Lorentz invariant. More often, one makes use of inclusive cross sections, when the interest is on the production of one specific particle type, regardless of the others, for instance as in $p + A \rightarrow \pi + X$, where X means the ensemble of all other produced particles. The inclusive cross section for this process is by definition:

$$E\frac{d^3\sigma}{dp^3} = \sum_n E_1 \frac{d^3\sigma}{dp_1^3} \int E_2 ... E_n \frac{d^3\sigma}{dp_2^3 ... dp_n^3} \tag{29}$$

The cosmic ray interactions (and shower development) are often described in the laboratory frame, where the target (air) nucleus is at rest and the primary projectile has 4-momentum $p \equiv (E_0, \vec{p})$. Therefore, remembering that the basic interaction is the nucleon-nucleon one, the corresponding center of mass energy (the one available for particle production) will be:

$$\sqrt{s} = \sqrt{m_p^2 + m_n^2 + 2m_n E_0} \sim \sqrt{2m_p^2 E_0} \tag{30}$$

regardless of the mass number A. We can verify that the knee region corresponds to about $\sqrt{s} = 1\ TeV$, while the $10^{17}\ eV$ range corresponds to the c.m. energy of the future LHC p-p collider at CERN ($14\ TeV$).

Looking at the gross feature of particle production in hadron interactions, the experiments show that the bulk of it consists of hadron emitted at limited transverse momentum with respect to the direction of the incident nucleon. ("soft" processes, with a typical $\langle P_t \rangle \sim 0.3\ GeV/c$, at low energy), which corresponds to the reciprocal of the transverse size of hadrons: in these processes the momentum transfer between the beam and target particles is small. More rarely, high-P_t production occurs ("hard" scattering), and this can be understood and calculated in the framework of perturbative QCD on the basis of the lowest order Feynman graphs involving the elementary constituents of hadrons (quarks and gluons)[32]. Unfortunately, there are not yet exact ways to calculate the bulk of soft, non-perturbative, interactions, and one has to rely on phenomelogical models. Some of them incorporate concepts deriving from the mathematical requirements of scattering theory, as unitarity and analicity, and also color flow and parton from general QCD. One example of these is the Dual Parton Model[33].

In any case, most of the energy is carried away longitudinally. It was initially suggested by Feynman that the inclusive cross sections could be expressed by a product of functions, factorizing the longitudinal part with a universal (energy independent) transverse momentum distribution.

$$E\frac{d^3\sigma}{dp^3} = F(\sqrt{s}, P_{long}) \cdot G(P_t) \tag{31}$$

Furthermore, also motivated by experimental results at low energy and in the framework of the description of hadrons as constituted by point-like elementary partons, he also suggested a scaling law for the longitudinal function, which should be a function of just one dimensionless variable, $x_{Feynman}$ or, simply x_F:

$$E\frac{d^3\sigma}{dp^3} = F(\sqrt{s}, P^{cm}_{long}) \cdot G(P_t) = F\left(x_F = 2P^{cm}_{long}/\sqrt{s}\right) \cdot G(P_t) \tag{32}$$

The exact definition of x_F would be $P^{cm}_{long}/(P^{cm}_{long})^{Max}$, and is defined from -1 to 1. In the high energy approximation, x_F, in the positive domain, can be approximated by $x_{lab} = E/E_{beam}$ disregarding terms of the order $\sqrt{p_T^2 + m^2}/\sqrt{s}$.

This scaling hypothesis is known as Feynman scaling[34], and provides interesting consequences, that we shall examine below. It is customary to describe the longitudinal distribution using another adimensional variable, y, called "rapidity":

$$y = \frac{1}{2}\log\left(\frac{E + P_{long}}{E - P_{long}}\right) \tag{33}$$

It has the advantage that a Lorentz boost corresponds to just an additional shift to the rapidity value defined in one reference frame. From the experimental point of view, say at colliders, it is also convenient because, in the relativistic range, we have $y \sim \eta = -log[tan\,(\theta/2)]$, where η is called "pseudo-rapidity", and θ is the angle of the produced particles as measured from the beam direction. We can re-express the invariant cross sections as:

$$E\frac{d^3\sigma}{dp^3} = \frac{d^3\sigma}{dy dp_T^2} \sim x_F \frac{d^3\sigma}{dx_F dp_T^2} \tag{34}$$

Where the last passage derives from the following approximate relation:

$$x_F \sim \frac{\sqrt{m^2 + P_t^2}}{\sqrt{s}} e^{y_{cm}} \tag{35}$$

Furthermore, the produced particles are found to be almost uniformly distributed in rapidity between some y_{min} and $y_{max} \propto \log s$. In the c.m. frame such a distribution is centered on $y = 0$. Under the strongest hypothesis of Feynman scaling (*i.e.* that $f(x_F = 0, P_t) =$ constant), the height of the plateau of the rapidity distribution is also constant and does not depend on energy. In that case the average multiplicity is expected to grow as $\langle n \rangle \propto \log s$. with σ_{inel}=constant. The Feynman scaling is never completely valid. and with increasing energy such hypothesis is more and more violated: the cross section grows, and so does the height of the rapidity plateau. Scaling violations now find their explanation in the contribution of hard QCD scattering as a function of energy[35]. However, the scaling hypothesis remains an useful attempt to understand the general behaviour of cosmic ray interactions. In fact, the relevant question for us is if such violations affect all the kinematic range useful for the description of cosmic ray production. In order to discuss that, let us establish some definition and the connections between x_F and y. The kinematic region around $y_{cm} = 0$ is called "central region" and it turns out to be the most affected by scaling violations.

Therefore, the central region in y corresponds to a very small region around $x_F = 0$. As $x_F \to 1$, we explore higher and higher rapidity regions, where in fact most of the energy flows. The kinematic region for which x_F exceeds ~ 0.1 is called "beam fragmentation" region (*i.e.* where secondary particles retain most of the momentum of the primary). Here, QCD scaling violations are predicted to be small, as can be seen from the results shown in Fig. 10. according to the Monte Carlo calculations of ref.[36]. This turns out to be the most important kinematic region for secondary cosmic ray production in the atmosphere. In the next section, we shall present some mathematical argument to show how this occurs.

Unfortunately, the high x_F distributions are experimentally measured only at lab energies of a few hundreds of GeV. In high energy hadron colliders, only the central region is generally inside the detector acceptance. Therefore, as far as high energy cosmic ray physics is concerned, we have to rely on the extrapolations to high x_F, under the guide of phenomenological models. However, it is a relevant experimental fact that the measurement of inclusive secondary cosmic ray fluxes at very high energy, like TeV muons, do indicate that the amount of Feynman scaling violation is small, as we will report with some additional detail in the last section.

There exists also the "target fragmentation" region, corresponding to $x_f \to -1$, but is it straightforward to understand that when boosting to the laboratory frame, we get from this region just low energy particles which are rapidly lost in the shower evolution.

From experiment we also learn that the simple hypothesis of factorization between longitudinal and transverse momentum is not true in reality: there is a non trivial correlation which makes $\langle P_t \rangle$ increase as a function of x_F, thus affecting the secondary production features in the most interesting (for us) kinematic region. Such correlation is known as "seagull" effect.

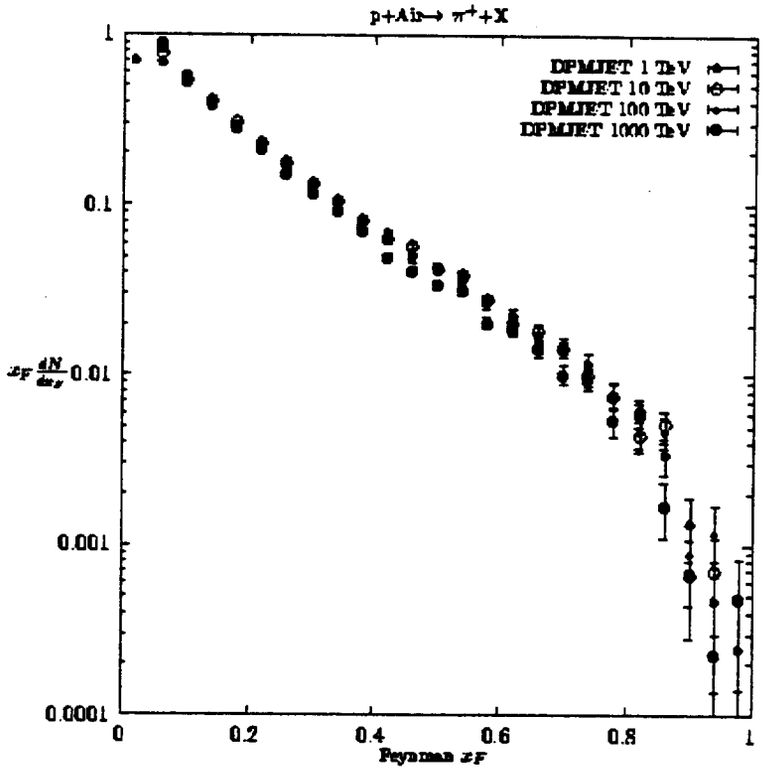

Figure 12: Calculated Feynman-x distribution for produced charged pions in proton-Air interactions at different laboratory energies.

Speaking about extrapolations, we have to go back to the question of the consequences of considering nuclei instead of free nucleons. Both experiments and phenomelogical models point out that pN interactions induce important modifications to the secondary production, as compared to the pp interactions at the corresponding c.m. energy. For instance, both multiplicity and transverse momentum distributions are affected by nuclear effects[37]. Also in this case there is a lack of useful experimental data, especially in the fragmentation region, and once again one has to rely on models.

In summary, the hadronic sector of high energy particle and nuclear physics, a part from the general acknowledgement of the centrality of color dynamics, is far from being successfully manageable as the electro-weak world. All this is surely a source of uncertainty, affecting the interpretation of indirect measurements in the field of cosmic rays. However, in our opinion, this fact should be also considered as an attractive opportunity to explore phenomena not yet accessed by accelerators.

7 Production of Secondary Particles in the Atmosphere

Before going in some details on the production of secondary particles, let consider the consequences of the structure of the hadronic interactions, in particular of the assumption of Feynman scaling, on the development of the shower. Within this approximation, the inelastic total cross sections, and hence the scattering lengths are constant and the average number of particles grows logarithmically with the energy. In this case, the shower production can be described as a process in which, when a particle crosses an interaction length, it interacts, producing an approximately constant number of secondaries per interaction. This schematization is similar to the one proposed in the thirties by Heitler for describing the formation of electromagnetic showers, and it is a trivial exercise to show that in this case the depth at which the shower arrives before being absorbed (which in this very schematic picture is the maximum depth) depends logarithmically on the energy of the primary.

If instead the multiplicity of secondary particles is the maximum kinematically allowed, namely all secondaries are produced at rest in the center of mass, which implies a multiplicity growing as $\sqrt{E}$, then (at fixed interaction length) the shower maximum is proportional to $\log(\log E)$, i.e. the shower develops completely and is absorbed after very few interaction lengths, with a very small probability to survive at observation level.

To go in better details, we present here an analytical treatment of the secondary particle production in atmosphere which is mainly derived from the textbook of T.K.Gaisser[2]. It is a uni-dimensional model, *i.e.* neglects the transverse structure of the showers (P_T=0), and is aimed to provide an expression for the inclusive fluxes of secondary cosmic rays.

The secondary particle propagation through the atmosphere can be described by a set of transport equations:

$$\frac{dN_i(E,X)}{dX} = -\left(\frac{1}{\lambda_i} + \frac{1}{d_i}\right) N_i(E,X) + \sum_j \int \frac{F_{ij}(E_i,E_j) N_j(Ej)}{E_i \lambda_j} dE_j \qquad (36)$$

where: X is the atmospheric depth in g/cm^2; $N_i(E,X)$ is the differential flux of particles of type i at depth X; λ_i is the interaction length of particle i at energy E; d_i is the decay length for particle i at energy E. The integral term describes the production mechanism of particle i from particle j, and

$$F_{ij}(E_i, E_j) \equiv E_i \frac{dn_i(E_i, E_j)}{dE_i} = \frac{dn_i(E_i, E_j)}{d\log E_i} \qquad (37)$$

that is the number of particles of type i produced in the energy range $E_i, dE_i + dE_i$ by a primary beam of energy E_j. These $F_{ij}(E_i, E_j)$ are obviously related to the inclusive production cross sections described in the previous section. In particular, if we work under the hypothesis of Feynman scaling validity, then:

$$F_{ij}(E_i, E_j) = F_{ij}(E_i/E_j) = F_{ij}(x_L) \simeq F_{ij}(x_F) = \frac{x_F}{\sigma} \frac{d\sigma}{dx_F} \qquad (38)$$

Furthermore, under this assumption we can consider λ as a constant.

Then, assuming heuristically to accept the validity of such Feynman scaling, and living in the uni-dimensional approach, we are left with a system of integro-differential equations which need the specification of boundary conditions. They can be one of the following two proposals:

1. give the flux at the top of the atmosphere, that is equivalent to fix the functional form of $N_i(E, X = 0)$. This kind of condition is suited for the description of the uncorrelated fluxes of particles irrespective of the primaries.

2. When it is appropriate to describe the production of secondary particles by a single primary, at a single energy, as for instance in the detailed discussion of the shower developement, then it can be convenient to give $N_i(E, X = 0) = A\delta(E - E_0/A)$. This is an expression of the superposition model.

For the first of two proposed conditions, it is possible to obtain analytical solutions, provided that a power law differential spectrum is given at the top of the atmosphere: $N_i(E, X = 0) = K_i E_i^{-(\gamma+1)}$. Then, we can look for separate variable solutions of the type $G(E)g(X)$. Let us discuss the production term. It becomes:

$$\begin{aligned} &\frac{g(X_v)}{\lambda_j} \int_{E_i}^{\infty} \frac{dE_j}{E_i} F_{ij}(E_i, E_j) G(E_i) \\ &\propto \int_{E_i}^{\infty} \frac{dE_j}{E_i} F_{ij}(E_i/E_j) E_j^{-(\gamma+1)} \\ &\propto \int_0^1 \frac{dx_F}{x_F^2} F_{ij}(x_F) \left(\frac{E_i}{x_F}\right)^{-(\gamma+1)} \\ &\propto E_i^{-(\gamma+1)} Z_{ij} \end{aligned} \tag{39}$$

where the functions $Z_{ij} \equiv \int_0^1 x_F^{\gamma-1} F_{ij}(x_F) dx$ are called "spectrum weighted" moments: they contain the complete information about the hadronic processes. Notice that, since $\gamma > 1$, the high x_F range of the inclusive cross sections are weighted much more than the central region near $x_F = 0$, where the weight is practically null; this intuitively correspnds to the fact that, with a fast falling spectrum, it is more likely for a secondary to retain as much as possible the energy of the primary. This is the reason why we say that the secondary cosmic ray production, from the hadronic physics point of view, is dominated by the fragmentation region.

Let us now examine the loss term in the transport equation, that is fundamental when we want to evaluate the inclusive flux of muons (coming from the decay of π and K) or neutrinos in the atmosphere. Here we learn immediately that we have a peculiar competition between decay and interaction probability.

$$\frac{dN_i}{dX} = -\left(\frac{1}{\lambda_i} + \frac{1}{d_i}\right) N_i \tag{40}$$

The question arises from the fact that when we express λ and d in the same units (g/cm^2), we have the exponential profile of the atmosphere to be taken into account, together with

the relativistic time expansion, considering that we work in the laboratory frame. Isolating the decay term, calling here $\gamma_i = E/m_i c^2$ the Lorentz factor, and τ the proper life-time, we can re-write the decay term, remembering that $\rho \equiv X_v/h_0$ and considering a generic slant depth $X = X_v/cos(\theta)$:

$$\frac{1}{d_i} = \frac{1}{\rho \gamma_i c\tau} = \frac{m_i c^2 h_o}{Ec\tau X cos(\theta)} = \frac{\epsilon_i}{EXcos(\theta)} \tag{41}$$

where $\epsilon_i = m_i c^2 h_0/c\tau$ is the "critical energy" for decay, . *i.e.* the energy above which a meson is more likely to interact than decay. For a charged pion $\epsilon_\pi \simeq 115\ GeV$, while for charged K it is around $850\ MeV$. We also learn that the larger the zenith angle, the larger is the length that a meson can travel in the atmosphere and the higher will be the probability to have enough time to decay. Here we can quote a few solutions for our transport problem:

a) Flux of nucleons in the atmosphere:

$$\frac{dN_n}{dXdE_n} = K_n E_n^{-(\gamma+1)} e^{-X/\Lambda} \tag{42}$$

In other words: nucleons attenuate exponentially, keeping their spectrum in energy. This last point is a direct consequence of Feynman scaling hypothesis. Here $\Lambda = \lambda_n/(1 - Z_{nn})$. This modification of the interaction length, in practice derives from the regeneration of nucleons in the atmosphere.

b) Flux of charged πs, in the high energy approximation:

$$\frac{dN_\pi}{dXdE_\pi} = K_\pi E_\pi^{-(\gamma+1)} \frac{Z_{n\pi}}{1 - Z_{nn}} \frac{\Lambda_\pi}{\Lambda_\pi - \Lambda_n} \left(e^{-X/\Lambda_\pi} - e^{X/\Lambda_n} \right) \tag{43}$$

where $\Lambda_\pi = \lambda_\pi/(1 - Z_{\pi\pi})$, and $\Lambda_{\pi n} = \lambda_n/(1 - Z_{\pi n})$. Again, charged mesons preserve the same power spectrum of primaries, with a longitudinal profile in atmosphere, peaking at a X_{max} value immediately obtainable from the above equation.

c) Muons. Here the decay term discussed above is crucial. A complete expression for the muon flux at sea level can be found in the quoted textbook[2]. We simply remind here two extreme cases: when $E_\mu << \epsilon_\pi$ then:

$$\frac{dN_\mu}{dE_\mu} \propto E_\mu^{-(\gamma+1)}; \quad \frac{dN}{dcos(\theta)} = const. \tag{44}$$

Instead, when $E_\mu >> \epsilon_\pi, \epsilon_K$ then

$$\frac{dN_\mu}{dE_\mu} \propto E_\mu^{-(\gamma+2)}; \quad \frac{dN}{dcos(\theta)} \propto \frac{1}{cos(\theta)} \tag{45}$$

The additional power in E, and the $cos(\theta)$ dependence reflect the consideration expressed above about the competition between decay and interactions of mesons.

In Fig. 11 we show the measured muon spectrum up to the TeV region (from ref.[2]). At high energy, the asymptotic $E_\mu^{-(\gamma+2)}$ behaviour seems to be well verified by experimental data. This could indirectly confirm the initial assumption of the existence of a substantial Feynman scaling in the fragmentation region.

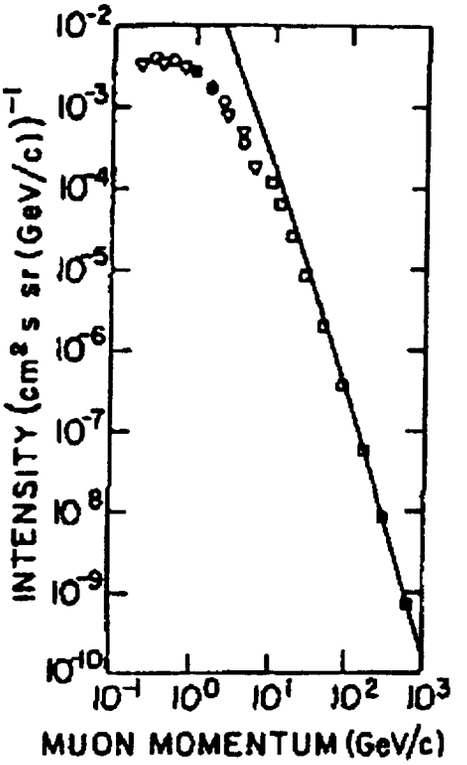

Figure 13: The differential muon flux at the bottom of atmosphere. The solid line represent the asymptotic power law expectation.

8 Acknowledgements

We are indebted to S. Parlati for precious discussions and assistance in preparing the lectures.

References

[1] M.S. Longair, *High Energy Astrophysics.* Cambridge University Press (1981).

[2] T.K. Gaisser, *Cosmic Rays and Particle Physics.* Cambridge University Press (1990).

[3] P. Sokolsky, *Introduction to Ultrahigh Energy Cosmic Ray Physics.* Addison-Wesley Publishing Company (1988).

[4] A.M. Hillas, *Cosmic Rays* Pergamon Press (1972).

[5] B. Rossi *High-energy Particles* (1952).

[6] V.L. Ginzburg and S.I. Syrovatskii, *The Origin of Cosmic Rays.* Pergamon Press (1964).

[7] A.S. Webster, *Astrophys. Lett* **5** (1970) 189.

[8] C.H. Tsao et al., *Astrophyis. Journal* **451** (1995) 275.

[9] D. Müller et al., *Astrophyis. Journal* **374** (1991) 356.

[10] For a general treatment see for instance: D.G. Wentzel *Ann. Rev. Astron. Atrophys* **12** (1974) 71.

[11] L.D. Landau and E.M. Lifshitz. *Fluid Mechanics* Pergamon Press (Oxford, 1982), pp. 315, 331.

[12] E. Fermi. *Phys. Rev.* **75** (1949) 1169.

[13] For a detailed discussion see P.O Lagage and C.J. Cesarsky. *Astron. Astrophys.* **118** (1983) 223 and **125** 249.

[14] There are recent upper limits on the emission of TeV gamma rays from Super Nova remnants reported at the 24th ICRC. For instance: C. Prosch at al. (HEGRA exp.), *Proc. of the 24th ICRC, Roma.* **2** (1995) 405; C. Prosch at al. (HEGRA exp.), *Proc. of the 24th ICRC. Roma.* **2** (1995) 471; A Borione et al, (CASA-MIA exp.), *Proc. of the 24th ICRC, Roma,* **2** (1995) 439; G.E. Allen et al, (CYGNUS exp.). *Proc. of the 24th ICRC, Roma,* **2** (1995) 443; R.W. Lenard et al, (Whipple obs.), *Proc. of the 24th ICRC. Roma.* **2** (1995) 475.

[15] P.L. Biermann, *Proc. of the 23rd ICRC, Invited. Rapporteur & Highlight Papers,* World Scientific (1994), 45.

[16] S. Swordy et al., *Nucl. Instr. & Meth.* **193** (1982) 591.

[17] T.H. Burnett et al., *Phys. Rev. Lett* **51** (1983) 1010.

[18] S. Swordy, *Proc. of the 23rd ICRC, Invited, Rapporteur & Highlight Papers*, World Scientific (1994), 243.

[19] B. Wiebel, Wuppertal University preprint (1994) WUB 94-08.

[20] S. Swordy, *Proc. of the 24th ICRC* **2** (1995) 697.

[21] A. Chiavassa, These proceedings.

[22] M.N. Dyakonov et al., *Proc. of the 20th ICRC* **6** (1987) 147.

[23] For a recent review: A.D. Erlykin, *Nuclear Phys. B (Proc. Suppl.)* **39A** (1995) 215.

[24] N. Chiba et al., *Nucl. Instr. & Meth.* **A311** (1992) 338.

[25] S. Yoshida et al, *Astroparticle Phys.* **3** (1995) 105.

[26] K. Greisen, *Phys. Rev. Lett* **16** (1966) 748; G.T. Zatsepin and V.A. Kuźmin, *Pisma Zh. Eksp. Teor. Fiz.* **4** (1966) 114.

[27] R.M. Baltrusaitis et al, *Nucl. Instr. & Meth.* **A240** (1985) 410.

[28] T.K. Gaisser et al., *Phys. Rev* **D47** (1993) 1919.

[29] O. Palamara, These proceedings.

[30] R.J Glauber and G. Matthiae, *Nucl. Phys.* **B21** (1970) 135.

[31] T. Hara et al., *Phys. Rev. Lett.* **50** (1983) 2058.

[32] For an introduction: F. Halzen and A.D. Martin *Quarks & Leptons: an Introductory Course in Modern Particle Physics*. John Wiley & Sons (1984).

[33] A. Capella et al., *Phys. Rev. Lett.* **58** (1987) 2015, and references therein.

[34] R.P. Feynman, *Phys. Rev.* **23** (1969) 1415.

[35] K. Alpgard et al., *Phys. Lett.* **B107** (1981) 310 and **B121** (1983) 209.

[36] G. Battistoni et al., *Astroparticle Phys.* **3** (1995) 157.

[37] For a discussion of the modification of pp cross sections due to nuclear effects inside a phenomelogical model see for instance C. Forti et al., *Phys. Rev.* **D42** (1990) 3668.